Regular article

A new class of high-entropy perovskite oxides

CrossMark

Sicong Jiang, Tao Hu [1], Joshua Gild, Naixie Zhou, Jiuyuan Nie, Mingde Qin, Tyler Harrington, Kenneth Vecchio, Jian Luo *

Department of NanoEngineering, University of California, San Diego, La Jolla, CA 92093, USA

ABSTRACT

A new class of high-entropy perovskite oxides (*i.e.*, multiple-cation solid solutions with high configurational entropies) has been synthesized. Six of the 13 compositions examined, including $Sr(Zr_{0.2}Sn_{0.2}Ti_{0.2}Hf_{0.2}Mn_{0.2})O_3$, $Sr(Zr_{0.2}Sn_{0.2}Ti_{0.2}Hf_{0.2}Nb_{0.2})O_3$, $Ba(Zr_{0.2}Sn_{0.2}Ti_{0.2}Hf_{0.2}Ce_{0.2})O_3$, $Ba(Zr_{0.2}Sn_{0.2}Ti_{0.2}Hf_{0.2}Y_{0.2})O_{3-x}$, $Ba(Zr_{0.2}Sn_{0.2}Ti_{0.2}Hf_{0.2}Nb_{0.2})O_3$ and $(Sr_{0.5}Ba_{0.5})(Zr_{0.2}Sn_{0.2}Ti_{0.2}Hf_{0.2}Nb_{0.2})O_3$, can form homogeneous single solid-solution phases. Goldschmidt's tolerance factor, instead of cation-size difference, influences the formation and temperature-stability of single cubic perovskite solid solutions. This new class of multicomponent (high-entropy) perovskite solid solutions with distinct and highly-tunable chemistries can enable simultaneous tailoring of multiple properties and potentially lead to new functionality.

© 2017 Acta Materialia Inc. Published by Elsevier Ltd. All rights reserved.

Recently, the research of high-entropy alloys (HEAs), also known as "multi-principal element alloys," has received great attentions because they possess a variety of excellent mechanical and physical properties [1–3]. The majority of HEAs are metals that have simple FCC, BCC or HCP structures [1–3]. To date, only a couple of high-entropy ceramic structures have been successfully fabricated in the bulk form. First, Rost et al. reported an entropy-stabilized rocksalt (FCC) oxide $(Mg_{0.2}Ni_{0.2}Co_{0.2}Cu_{0.2}Zn_{0.2}O)$ in 2015 [4] and its derivative materials doped with Li and Ga cations showed promising ion-conducting and dielectric properties [5,6]. Second, high-entropy metal diborides with a layered AlB_2 crystal structure, which contains alternating 2-D high-entropy cationic/metallic solid-solution layers and covalent boron nets, were synthesized as a new class of ultra-high temperature ceramics [7]. In this study, we successfully synthesized, for the first time to our knowledge, yet another new class of high-entropy perovskite oxides, which can potentially have unique physical properties and allow simultaneous tailoring of multiple physical properties due to their distinct and highly-tunable chemistries. This study also represents the first report of high-entropy materials that have a complex ionic crystal structure with at least two cation sublattices.

An ABO_3 perovskite oxide contains a 12-fold coordinated A cation sublattice, a 6-fold coordinated B cation sublattice, and an octahedral oxygen anion sublattice. In 1926, Goldschmid introduced a structural "tolerance factor" [8] to predict the stability of perovskite:

$$t = \frac{R_A + R_O}{\sqrt{2}\,(R_B + R_O)} \qquad (1)$$

where R_A, R_B and R_O, respectively, are the radii of A cation, B cation and oxygen anion. A cubic phase is likely stable if $0.9 \le t \le 1.0$, while a hexagonal or tetragonal phase may form if $t > 1.0$ and an orthorhombic or rhombohedral phase may form if $t < 0.9$ [9]. ABO_3 perovskite oxides have excellent and diverse physical properties for applications in many different areas, *e.g.*, they can be used as cathode materials for solid oxide fuel cells [10], proton conductors [11], photocatalysts [12], dielectrics [13–16], and ferroelectric and multiferroic materials [17–21]. They can also serve as the base crystal structure for realizing 2-D electron gas and high-temperature superconductivity [16,22–24]. Doping with multiple cations may allow simultaneous tailoring of multiple physical properties of ABO_3 perovskite oxides to meet challenging requirements of real applications, as exemplified by a couple of recent studies for fuel cells [25–27]. In this study, we further extend ABO_3 perovskite solid solutions to high-entropy compositions, where we successfully synthesized six single-phase, high-entropy, perovskite oxides (among 13 compositions that we have examined; Table 1), *i.e.*, $Sr(Zr_{0.2}Sn_{0.2}Ti_{0.2}Hf_{0.2}Mn_{0.2})O_3$, $Sr(Zr_{0.2}Sn_{0.2}Ti_{0.2}Hf_{0.2}Nb_{0.2})O_3$, $Ba(Zr_{0.2}Sn_{0.2}Ti_{0.2}Hf_{0.2}Ce_{0.2})O_3$, $Ba(Zr_{0.2}Sn_{0.2}Ti_{0.2}Hf_{0.2}Y_{0.2})O_{3-x}$, $Ba(Zr_{0.2}Sn_{0.2}Ti_{0.2}Hf_{0.2}Nb_{0.2})O_3$ and $(Sr_{0.5}Ba_{0.5})(Zr_{0.2}Sn_{0.2}Ti_{0.2}Hf_{0.2}Nb_{0.2})O_3$, and we have further shown that the Goldschmidt's tolerance factor correlates with the formation and temperature-stability of these multi-cation perovskite solid-solution phases.

Table 1

Summary of the key findings of all 13 compositions examined. To roughly indicate the amounts of secondary phases, "trace" means that a secondary phase could not be identified by XRD but EDXS mapping show composition non-uniformity. If a secondary phase can be detected by XRD and the intensity of its strongest XRD peak is <6% of that of the perovskite (110) peak, we label "minor" in the table; otherwise, "major" implies that the intensity ratio of the maximum XRD peaks is >6%.

	Composition	Secondary phase?			$\delta(R_B)$	Tolerance factor t
		1300 °C	1400 °C	1500 °C		
#S0	$Sr(Zr_{0.25}Sn_{0.25}Ti_{0.25}Hf_{0.25})O_3$	Minor	Minor	Major	6.7%	0.97
#S1	$Sr(Zr_{0.2}Sn_{0.2}Ti_{0.2}Hf_{0.2}Mn_{0.2})O_3$	Minor	Trace	No	11.2%	0.99
#S2	$Sr(Zr_{0.2}Sn_{0.2}Ti_{0.2}Hf_{0.2}Ce_{0.2})O_3$	Major	Major	Major	11.9%	0.95
#S3	$Sr(Zr_{0.2}Sn_{0.2}Ti_{0.2}Hf_{0.2}Y_{0.2})O_{3-x}$	Major	Minor	Trace	13.3%	0.95
#S4	$Sr(Zr_{0.2}Sn_{0.2}Ti_{0.2}Hf_{0.2}Ge_{0.2})O_3$	Trace	Trace	Major	11.2%	0.99
#S5	$Sr(Zr_{0.2}Sn_{0.2}Ti_{0.2}Hf_{0.2}Nb_{0.2})O_3$	Minor	Trace	No	6.0%	0.97
#B0	$Ba(Zr_{0.25}Sn_{0.25}Ti_{0.25}Hf_{0.25})O_3$	Minor	Minor	Major	6.7%	1.03
#B1	$Ba(Zr_{0.2}Sn_{0.2}Ti_{0.2}Hf_{0.2}Mn_{0.2})O_3$	Major	Major	Major	11.2%	1.05
#B2	$Ba(Zr_{0.2}Sn_{0.2}Ti_{0.2}Hf_{0.2}Ce_{0.2})O_3$	No	Minor	Major	11.9%	1.01
#B3	$Ba(Zr_{0.2}Sn_{0.2}Ti_{0.2}Hf_{0.2}Y_{0.2})O_{3-x}$	No	Major	Major	13.3%	1.01
#B4	$Ba(Zr_{0.2}Sn_{0.2}Ti_{0.2}Hf_{0.2}Ge_{0.2})O_3$	Minor	Minor	Major	11.2%	1.05
#B5	$Ba(Zr_{0.2}Sn_{0.2}Ti_{0.2}Hf_{0.2}Nb_{0.2})O_3$	No	Minor	Major	6.0%	1.03
#$S_{0.5}B_{0.5}$5	$(Sr_{0.5}Ba_{0.5})(Zr_{0.2}Sn_{0.2}Ti_{0.2}Hf_{0.2}Nb_{0.2})O_3$	Minor	No	No	6.0%	1.00

We note that there are several definitions of high-entropy alloys [2], which may or may not be entropy-stabilized phases; here, we use the term "high-entropy" to refer to solid solutions that have high configuration entropies (specifically, ≥1.5R per mole, where R is the gas constant, following a definition used by Miracle et al. [28]).

Specifically, we partially substituted Ti of $SrTiO_3$, $BaTiO_3$ and $(Sr_{0.5}Ba_{0.5})TiO_3$ with several elements of equal molar fractions (1/4 or 1/5), selected from Zr, Sn, Hf, Mn, Nb, Ce, Ge and Y. Thirteen targeted compositions were selected and studied (Table 1). To synthesize specimens, appropriate amounts of purchased oxides were weighed to match the stoichiometry of the 13 targeted compositions (Supplementary Table S-I). The powders were blended and high energy ball milled (HEBM) in a Si_3N_4 vial in a SPEX 8000D mill for 6 h. To prevent overheating, the HEBM was stopped every 30 min to rest for 10 min. The milled powders were compacted into pellets in a 1/4 inch-diameter die at ~300 MPa (for ~120 s). The pellets were sintered in a tube furnace isothermally (5 °C/min ramp rate). Subsequently, most sintered specimens were cooled inside the furnace (power off), where the cooling rate was measured to be about 50 °C/min at 1500 °C and 10 °C/min at 1300 °C. Specimens were characterized by X-ray diffraction (XRD) utilizing a Rigaku diffractometer with Cu Kα radiation and scanning electron microscopy (SEM, FEI Phillips XL30) equipped with an energy dispersive X-ray spectroscopy (EDXS) detector. Selected specimens were characterized by aberration-corrected scanning transmission electron microscopy (AC STEM) using a 200 kV JEOL ARM-200F STEM with a CEOS Gmbh probe Cs corrector, for which TEM specimens were prepared by using a dual-beam FEI Scios focused ion beam (FIB).

We have investigated Composition #S1, $Sr(Zr_{0.2}Sn_{0.2}Ti_{0.2}Hf_{0.2}Mn_{0.2})O_3$, as our primary model system. XRD revealed the presence of a secondary phase in the specimen sintered at 1300 °C (Fig. 1(a)). With increasing sintering temperature, the amount of the secondary phase decreased. The $Sr(Zr_{0.2}Sn_{0.2}Ti_{0.2}Hf_{0.2}Mn_{0.2})O_3$ specimen sintered at 1500 °C exhibited a single cubic phase, with no trace of the secondary phase detectable by XRD (Fig. 1(a)) and EDXS elemental mapping (Fig. 1(b)). Fig. 1(b) shows that a Mn-enriched secondary phase was detected from the EDXS mapping in the specimen sintered at 1400 °C (for 10 h and furnace-cooled, as a standard sintering recipe adopted in this study), while this secondary phase was not detectable by XRD (Fig. 1(a)). To verify that this secondary phase formed at 1400 °C was not kinetically limited, we conducted two additional experiments (Fig. 1(c)). While a specimen sintered at 1500 °C for 2 h and air-quenched was homogeneous, this Mn-enriched phase precipitated out in the 1500 °C × 2 h + 1400 °C × 2 h specimen (Fig. 1(c)). The dissolution of the Mn-enriched secondary phase in the homogenous cubic perovskite solid solution at a higher temperature of 1500 °C may be explained as entropy driven; however, we also found that precipitation occurred at a higher temperature of 1500 °C in several Ba based multi-

cation perovskites that were single phases at lower temperatures (Table 1). Thus, it is uncertain whether entropy is the main driving force for the precipitation/dissolution of secondary phases in these multi-cation perovskite solid solutions.

To further confirm the formation of the disordered solid solution perovskite phase, we also calculated the XRD pattern based on the standard kinematic diffraction theory and assuming equal and random
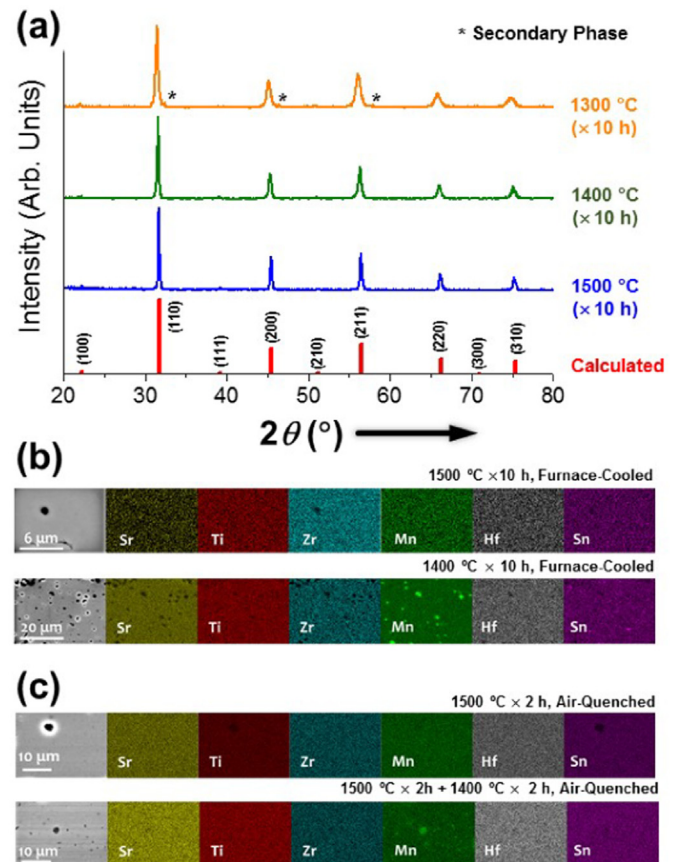
Fig. 1. (a) XRD patterns of $Sr(Zr_{0.2}Sn_{0.2}Ti_{0.2}Hf_{0.2}Mn_{0.2})O_3$ (Composition #S1) specimens sintered at different temperatures (isothermally for 10 h and furnace-cooled), along with a calculated XRD pattern assuming equal and random occupations of five cations on the B lattice site of a high-entropy perovskite crystal structure. Cross-sectional EDXS elemental maps of (b) selected standard sintered specimens (corresponding to those shown in (a)) and (c) air-quenched specimens to show that the Mn-enriched secondary phase formed at 1400 °C was not kinetically limited. (For interpretation of the references to color in this figure, the reader is referred to the web version of this article.)